18TH WORLD CONFERENCE ON EARTHQUAKE ENGINEERING
WCEE2024
MILAN

MILAN, ITALY
30TH JUNE - 5TH JULY 2024

www.wcee2024.it

EFFECTS OF NON-LINEAR SOIL BEHAVIOUR ON THE SEISMIC RESPONSE OF MULTI-STOREY SHALLOW UNDERGROUND STRUCTURES

M. Zucca[1], G. Tropeano[1] & F.M. Soccodato[1]

[1] Department of Civil, Environmental Engineering and Architecture, University of Cagliari, Via Marengo 2, 09123, Cagliari, Italy, giuseppe.tropeano@unica.it

Abstract: *The assessment of the seismic behaviour of underground structures is one of the most current research topics in seismic geotechnical and structural engineering due to the complex soil-structure interaction phenomena that are involved. In the last decades, several numerical approaches, more or less simplified, have been developed to evaluate the seismic behaviour of these structures, especially following the significant damage observed after recent strong earthquakes. In parallel, the International Codes have begun to address to the concepts of seismic design. Despite the significant progress made, several uncertainties remain regarding the correct representation of the seismic behaviour of underground structures. The paper presents the main results of nonlinear analyses performed to evaluate the seismic behaviour of a multi-storey, shallow underground structure embedded in coarse grained soils varying seismic intensity. The results are compared with those obtained for the same models using linear model both for soil and structure behaviour, in order to assess the influence of the non-linearity of the seismic response on the magnitude of the stresses acting on the concrete retaining walls.*

1. Seismic behavior of underground structures: overview and some open issues

Over last decades, classifications of different types of underground structures have been proposed based on construction method (Bickel 2006) and intended use. Despite these differences in terms of construction method and structural characteristics, the seismic behaviour of these structures is governed by similar parameters. It is possible to classify the damaging effects of strong earthquakes on underground structures into two main groups: (i) damage due to ground shaking and (ii) damage due to ground failures. As a result of the seismic waves generated by an earthquake, the soil will be subjected to vibrations that are manifested as soil shaking: consequently, underground structures will suffer deformations more or less simultaneously with the surrounding soil deformations. The second group includes different types of soil failure, such as faulting and tectonic uplift, subsidence and slope instability.

However, for a long period, underground structures were considered to be virtually invulnerable to earthquakes. This speculation on the safety of underground structures has changed after some of them suffered serious damage caused by strong seismic events, including the 1995 Kobe (Japan), 1999 Chi-Chi (Taiwan) and 1999 Kocaeli (Turkey) earthquakes, especially in the case of inadequate seismic design, as reported in Hashash et al. (2001). In particular, the failure of Daikai subway station (Figure 1), which occurred during the 1995 Kobe earthquake, was emblematic: the central columns collapsed because they were designed considering only vertical loads (Iida et al. 1996, Kawashima 2000, Hashash et al. 2001).

During the last decades, the seismic behaviour of underground structures has been the subject of several studies as Dowding and Roze (1978), Owen and Scholl (1981), Yoshikawa and Fukuchi (1984), Sharma and Judd (1991), Power et al. (1998), Kawashima (2000), Wang (2001), Wang (2009), Hashash et al. (2001), Kontoe et al. (2008).

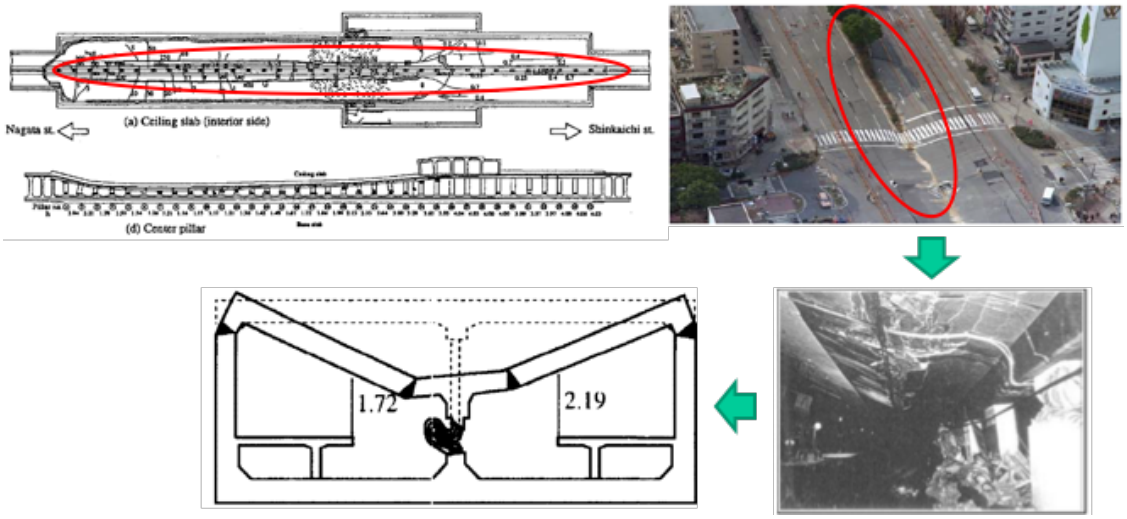

Figure 1. Daikai station collapse mechanism.

In addition, several Technical Codes have started to pay attention to the seismic design of underground structures, and in the same way, different methods have been developed to evaluate the seismic response of such structures in the transverse (Wang 1993, Penzien and Wu 1998, Penzien 2000, JRA 1992, ISO 2005, Hoeg 1968, Bobet 2003, Bobet 2010, Park et al 2009) and longitudinal (Kuesel et al. 1976, St, John and Zahrah 1987, Kiyomiya 1995) directions, including coupled and decoupled approaches. Furthermore, some comparisons between the different proposed methods have been carried out (Gomez-Masso and Attala 1984). In Andreotti e Lai 2015, a procedure to obtain the fragility curves for the evaluation of the seismic performance of underground structures has been proposed.

Despite these significant progress, many uncertainties persist. These regard mainly the aspects related to the complexity of the soil-structure interaction phenomena. In fact, this research topic is not adequately addressed by current standards, especially when dealing with structures featuring more than two horizontal restrains.

2. Sensitivity analysis

To evaluate the seismic behavior of a shallow multi-propped underground structure, a sensitivity analysis has been carried out considering different values of the shear modulus (related to the shear wave velocity) of the soil where the structure is embedded (Figure 2). In particular, the structure is considered embedded in a dry, coarse grained soil.

The subsoil considered in this study is constituted by a 31.6 m thick layer of coarse grained soil resting above a 51.30 m thick layer of sandstone as bedrock. (Figure 3). The soil is characterized by a shear wave velocity ranging between 360 and 750 m/s. The main mechanical properties of the soil profiles are summarized in Table 1.

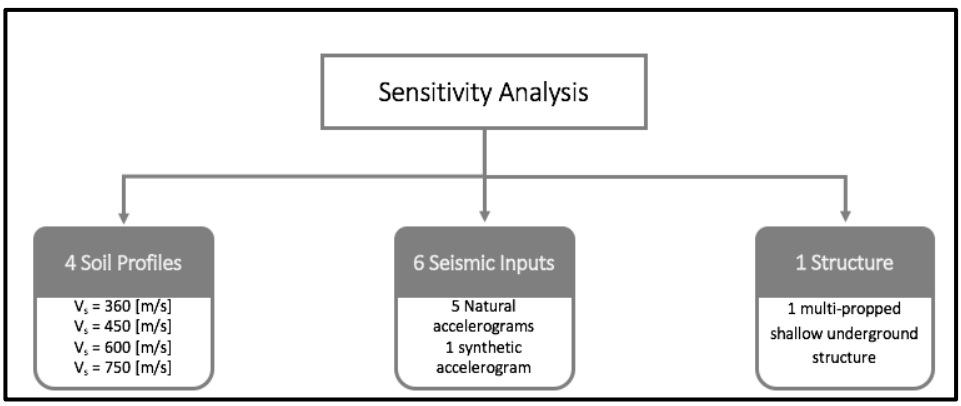

Figure 2. Sensitivity analysis schematic sequence.

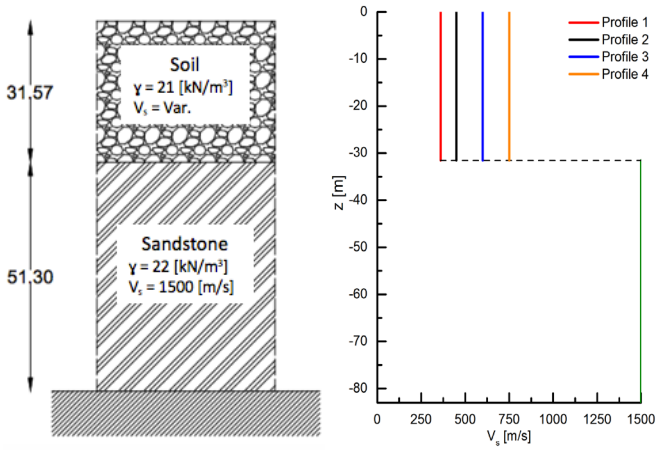

Figure 3. Soil model and related shear wave velocity profile.

Table 1. Mechanical properties of the four soil profiles.

Soil profile [n°]	Unit weight (γ)[kN/m³]	Cohesion (c')[kPa]	Friction angle (φ')[°]	Dilatancy Angle (ψ) [°]	Shear wave velocity (V_s)[m/s]	Poisson ratio (ν) [-]
1	21	40	39	0	360	0.3
2	21	40	39	0	450	0.3
3	21	40	39	0	600	0.3
4	21	40	39	0	750	0.3

The seismic response of the underground structures is strictly related to the behaviour of the surrounding soil; for a given seismic input, the possible occurrence of resonance effects when the fundamental frequencies of the soil column are close to the frequencies of the seismic input characterized by the maximum energy content plays a major role. In this study, 5 seismic accelerogram components recorded during 5 different European strong earthquakes (Greece, Amatrice, L'Aquila, Friuli and Montenegro) included in the European Strong Motion Database and 1 accelerogram generated analytically using the seismic characteristics of Lima city in Peru for the new line 2 metro design have been used. Table 2 reports the main properties of the considered seismic inputs, where PGA is the peak ground acceleration, PGV is the peak ground velocity and PGD indicates the peak ground displacement.

In particular, the accelerograms have been selected within a Magnitude (Mw) ranging between 6 and 7 and a PGA value between 0.35 g and 0.53 g. The inputs are characterized by different values of integral parameters, gaining a large variability of the ground motion characteristics. The seismic inputs have been applied both unscaled and scaled (only in terms of PGA, while keeping unchanged the frequency content of the seismic signals) considering a PGA value ranging between 0.13 and 0.22 g. Figures 4 and 5 shown the seismic signals and the related representation in the frequency domain highlighting the relation between the signal frequency content and the fundamental natural frequencies of the four soil columns listed in Table 3.

Table 2. Main characteristics of the seismic inputs.

Event [-]	Date [-]	Hour [-]	Magnitude (M_w) [-]	Station [-]	Component [-]	PGA [g]	PGV [cm/s]	PGD [cm]	Arias Intensity [cm/s]
Greece	15/06/1995	01:49 AM	6.5	AIGA	TRAN	0.52	51.3	8.3	117.1
Amatrice	30/10/2016	07:30 AM	6.5	AMT	E-W	0.53	37.9	7.5	156.4
L'Aquila	06/04/2009	03:32 AM	6.1	AQG	N-S	0.49	35.8	6.0	132.4
Friuli	06/05/1976	09:00 PM	6.0	FRC	N-S	0.35	23.7	5.3	84.5
Montenegro	15/04/1979	06:19 AM	6.9	PETO	N-S	0.45	38.5	6.9	455.7
Lima	2017	-	8.1	-	-	0.50	125.5	449.0	1492.0

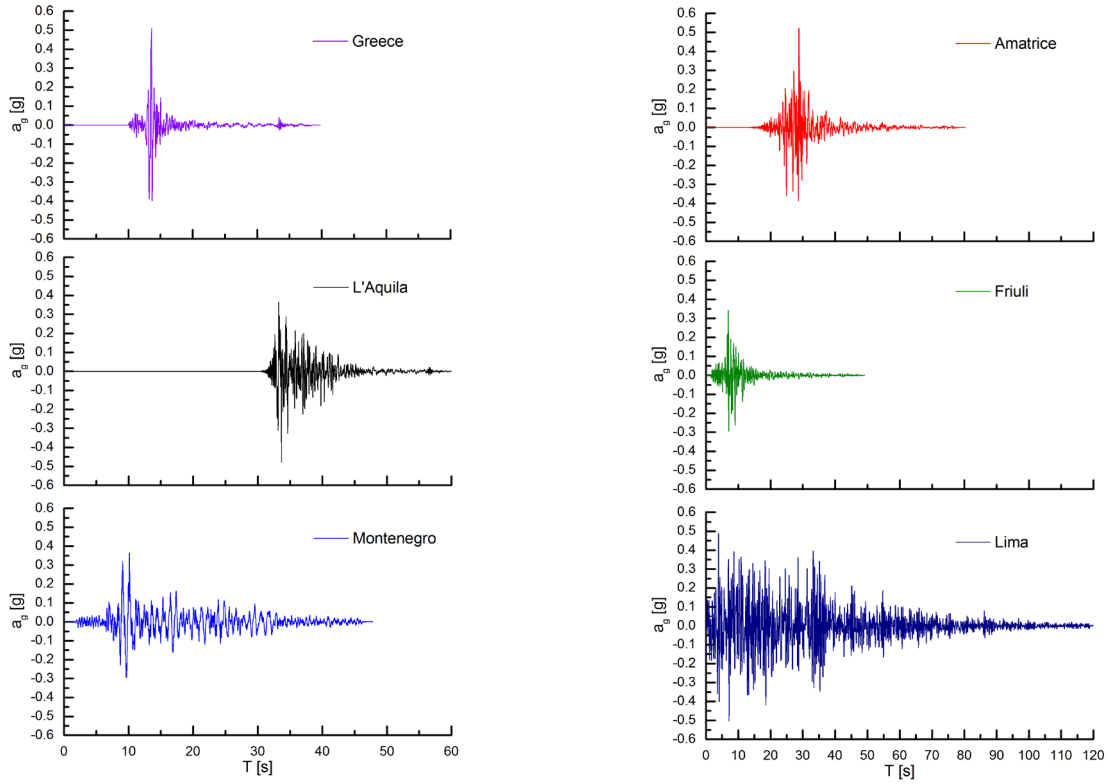

Figure 4. Seismic inputs.

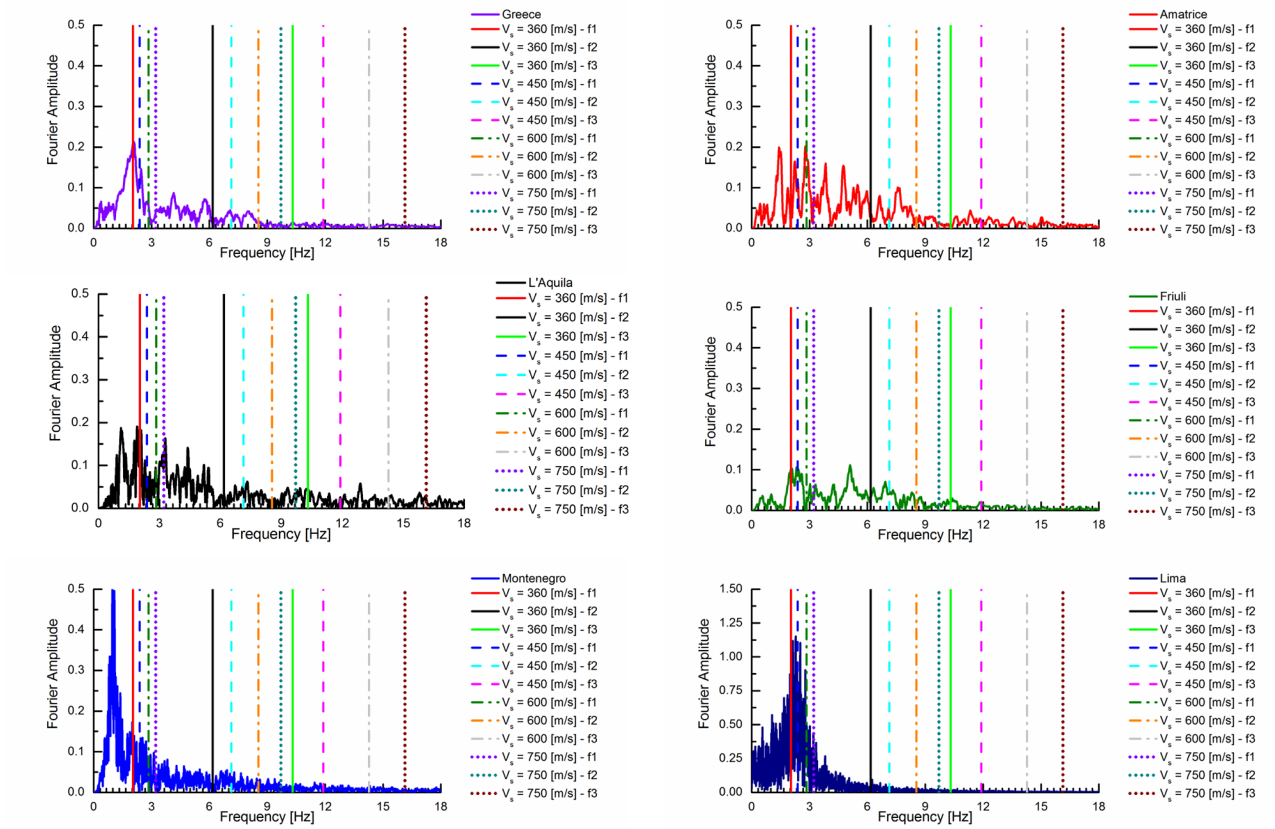

Figure 5. Seismic inputs in frequency domain.

Table 3. Soil columns fundamental frequencies.

Soil profile (V_s) [m/s]	T_1 [s]	T_2 [s]	T_3 [s]
360	0.490	0.162	0.097
450	0.420	0.140	0.084
600	0.350	0.117	0.070
750	0.310	0.103	0.062

The relation between the frequency content of the different seismic signals and the main natural frequencies of the soil columns is fundamental to understand the possible occurrence of resonance effects. It is possible to notice that the peaks of the Fourier transform of the six seismic events are located near the frequencies range that involve the first fundamental frequency of the four soil profiles except for Montenegro seismic input.

The shallow underground used in this work is characterized by a rectangular plan having dimensions equal to 132.16 m × 29.00 m. The main structural elements are the reinforced concrete (RC) retaining walls having a thickness equal to 1 m and the circular RC columns characterized by a diameter equal to 1.2 m arranged according to a rectangular grid of 14.70 m × 12.00m. The foundations of the columns are realized by circular RC piles with a diameter equal to 1.8 m and 9 m deep (Figure 6).

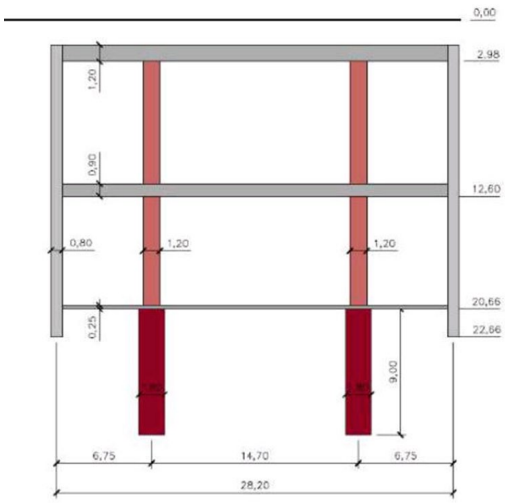

Figure 6. scheme of the shallow underground structure considered in this study (dimensions in meters).

Table 4 summarizes the mechanical properties of the materials which that characterize the main structural elements of the metro station.

Table 4. Materials mechanical properties.

Structural elements	Concrete (f_{ck}) [MPa]	Steel (f_{yk}) [MPa]
Columns	40	420
Piles	40	420
Retaining Walls	30	420
Slabs	40	420

3. Numerical modelling

The non-linear dynamic analysis of the system has been carried out, considering plane strain conditions, using the finite difference commercial software FLAC^{2D} (Itasca 2007). The implemented computational grid has dimensions 208.20 m × 83.87 m. An elastic perfectly plastic constitutive law with a Mohr Coulomb strength rule for the soil profile has been used, while a simple elastic model has been chosen for the sandstone. The shear stiffness at small strain (G_0) has been computed as a function of the shear wave velocity. The soil hysteretic behavior has been considered through the application of the shear modulus decay curves proposed by Seed and Idriss 1970 and Stokoe et al. 2013. The hysteretic damping is taken into consideration using the generalized Masing rules. The maximum size of the computation mesh elements has been defined to allow the proper propagation of harmonics with 18 Hz frequency, that is the maximum frequency of the seismic signals adopted in this research work, according to Kuhlemeyer and Lysmer 1973. The size of the mesh elements is optimized using the relation reported in Pagliaroli et al. 2007. To avoid the reflection effects on the vertical lateral boundaries of the computational grid, free-field boundary conditions available in FLAC^{2D} library have been applied. The dynamic analysis has been carried out applied the selected time histories at the base of the computational grid considering a value of damping of the sandstone layer equal to 1%.

4. Seismic response of the system

As reported in Soccodato and Tropeano 2015, the ground motion response obtained by the execution of the sensitivity analysis, is influenced by several overlapping effects such as: (i) the different characteristics of the soil columns, (ii) the non-linear behavior of the soil and (iii) the geometry of the system.

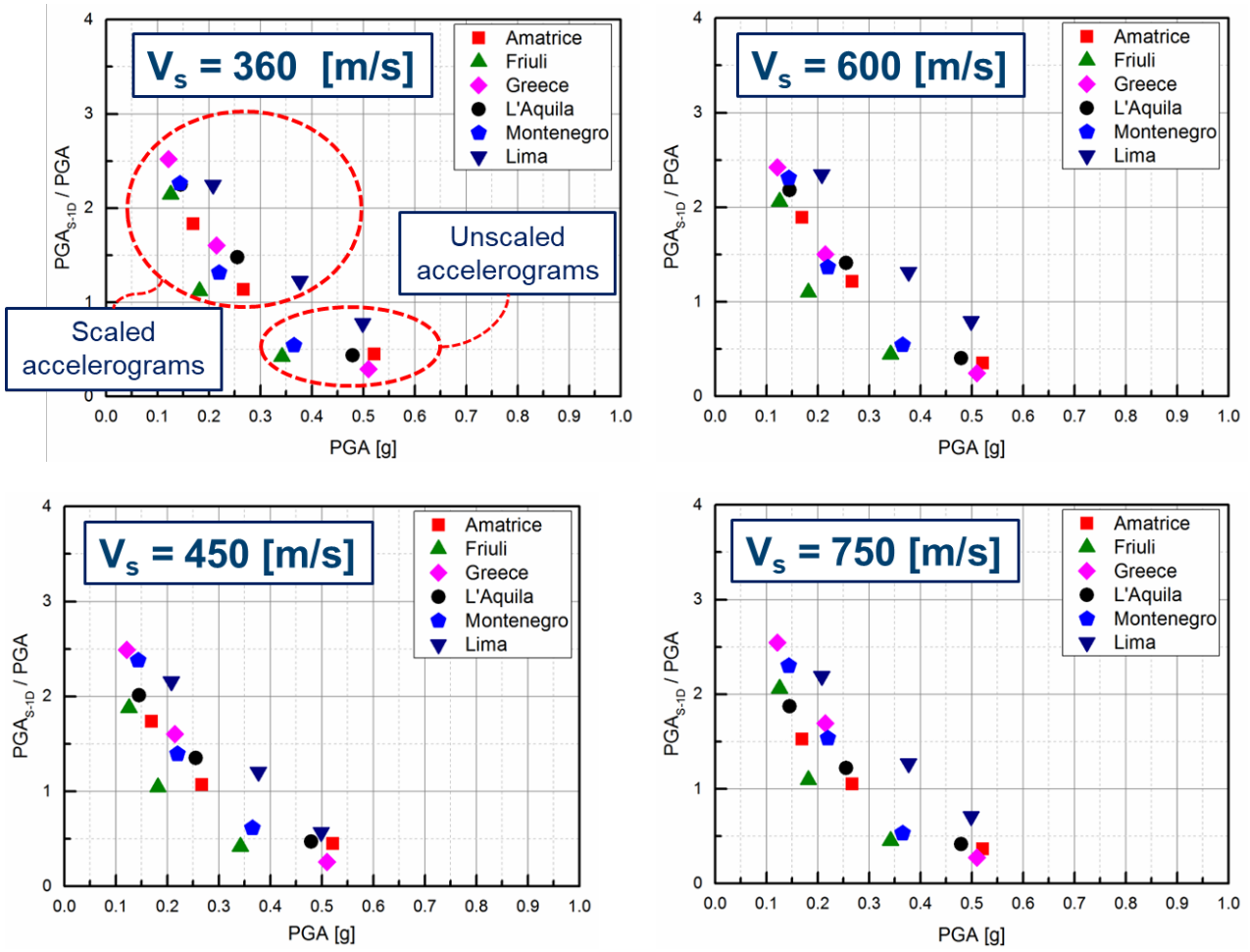

Figure 7. 1D response factor.

The results of the free-field analysis (in 1D condition for the scheme considered in this work) expressed in terms of ratio between the maximum acceleration evaluated at ground level in free field condition ($PGA_{S\text{-}1D}$) and the maximum acceleration which characterize the considered time history (PGA) are shown in Figure 7.

The soil response is conditioned by the system vibration modes excited by the different seismic signals. In fact, the seismic response of the soil column is strictly influenced by the soil motion and straining due to the markedly non-liner behavior of the soil.

The resonance effects with the first vibration mode of the different soil profiles lead to an increase of the shear strain in the deepest soil layers and, consequently, additional damping appear as a function of the strongly non-linear behavior of the soil. For these reasons, the free-field analysis results are characterized by a larger amplification of the peak acceleration. Only considering the unscaled accelerograms, the free-field analysis shows a decrease of the value of the peak acceleration due to the seismic signals characteristics which enhance the dissipation effects of the soil due to its non-linear behavior.

5. Decoupled approach

To evaluate the seismic performance of the underground structure described in Section 2, a decoupled approach has been used. In particular, the decoupled approach applied in this research work is based on the evaluation of the soil deformations without taking into account the presence of the structure and in the application of such deformations (calculated at the depth of the structure) to the structure, according to the procedure illustrated in Figure 8.

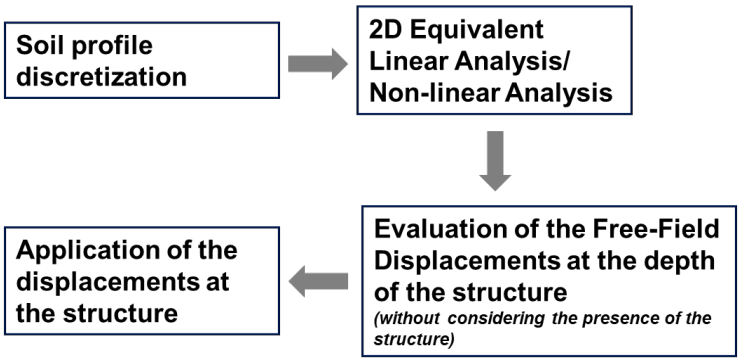

Figure 8. Decoupled approach.

To evaluate the seismic response of the soil profiles in order to obtain the displacements at both the top and the base of the structure, two different types of approach have been applied. In the first approach, the soil profiles discretization has been implemented using Deepsoil software code, developed by Hashash et al. 2016, to perform equivalent linear analysis. Also in such a case, the degradation of the soil shear modulus has been considered through the decay curves given by Seed and Idriss 1970 and Stokoe et al. 2013. In Figure 9 it is possible to see an example of displacements trend obtained for the soil profile characterize by a value of shear wave velocity equal to 360 m/s subject to Montenegro seismic input (the solid line indicates the displacements profile starting from the depth of the structure base.

The displacement distributions obtained for the other soil profiles subjected to the different seismic inputs follows the same trend, resulting from the first vibration mode shape of the soil columns. These results are in accordance with that reported in previous Section 4, where it is clear how the seismic inputs mainly excite the first fundamental frequency of the soil columns. Furthermore, it is evident that the displacements obtained at the ground level significantly decrease when the stiffness of the soil profile increases.

Table 5 summarizes the main results obtained from the execution of equivalent linear analysis expressed in terms of relative displacements obtained as the difference between the displacements evaluated at the top and at the base of the RC retaining walls of the underground structure.

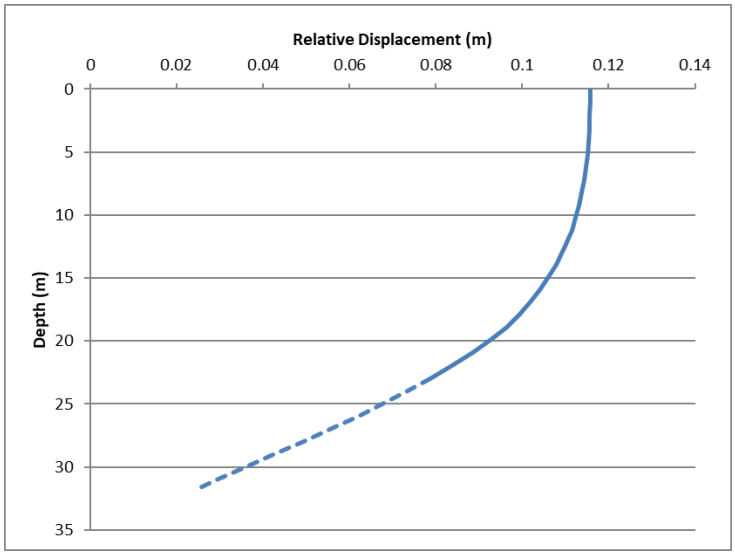

Figure 9. Displacements trend of the soil profile with V_s = 360 m/s under Montenegro seismic input.

Table 5. Relative displacements obtained from the equivalent linear analysis.

Soil profile (V_s) [m/s]	Amatrice [mm]	Friuli [mm]	Greece [mm]	Montenegro [mm]	L'Aquila [mm]	Lima [mm]
360	13	8	28	37	15	34
450	11	5	27	7	8	23
600	5	2	3	2	2	6
750	2	2	1	1	2	1

The maximum increment of bending moment due to the seismic load and acting on the section of the RC retaining walls located in correspondence to the central slab, is calculated starting from the static condition. Table 6 shows that the maximum increase is obtained for the soil profile having shear wave velocity equal to 360 m/s. In particular, the results of the equivalent linear analysis indicate that the maximum increase of bending moment is equal to 110 kNm in the case of Montenegro seismic input, while the bending moment increase due to the seismic action is almost negligible in the cases of soil profiles characterized by high values of stiffness (V_S = 600 m/s and V_S = 750 m/s).

In the second approach, the free-field displacements obtained using the numerical model described in Section 3 and performing the non-linear analysis have been considered. Table 7 reports the main results obtained these analyses in terms of relative displacements obtained as the difference between the displacements evaluated at the top and at the base of the RC retaining walls of the underground structure.

Table 8 reports the values of bending moment obtained from the non-linear analysis Also in this approach the maximum increment of bending moment due to seismic action is obtained for the soil profile characterized by low values of shear wave velocity and it is equal to 357 kNm in the case of Lima seismic input.

Table 6. Equivalent linear analysis: bending moment acting in the considered section.

Soil profile (V_s) [m/s]		Montenegro	L'Aquila	Greece	Friuli	Amatrice	Lima
360	Static (M_0) [kNm]	518	518	518	518	518	518
	Seismic (M) [kNm]	628	562	601	542	557	619
	Δ [%]	21	9	16	5	7	20
450	Static (M_0) [kNm]	451	451	451	451	451	451
	Seismic (M) [kNm]	472	475	532	466	466	520
	Δ [%]	5	5	18	3	3	15
600	Static (M_0) [kNm]	370	370	370	370	370	370
	Seismic (M) [kNm]	376	376	379	376	376	387
	Δ [%]	2	2	2	2	2	5
750	Static (M_0) [kNm]	312	312	312	312	312	312
	Seismic (M) [kNm]	315	318	315	318	318	315
	Δ [%]	1	2	1	2	2	1

Table 7. Relative displacements obtained from the non-linear analysis.

Soil profile (V_s) [m/s]	Amatrice [mm]	Friuli [mm]	Greece [mm]	Montenegro [mm]	L'Aquila [mm]	Lima [mm]
360	18	12	33	42	19	120
450	16	8	30	13	10	107
600	8	4	7	4	4	36
750	5	3	2	2	4	23

Table 8. Non-linear analysis: bending moment acting in the considered section.

Soil profile (V_s) [m/s]		**Montenegro**	**L'Aquila**	**Greece**	**Friuli**	**Amatrice**	**Lima**
360	Static (M_0) [kNm]	518	518	518	518	518	518
	Seismic (M) [kNm]	643	574	616	554	571	875
	Δ [%]	24	11	19	7	10	69
450	Static (M_0) [kNm]	451	451	451	451	451	451
	Seismic (M) [kNm]	490	481	541	475	499	769
	Δ [%]	9	7	20	5	11	71
600	Static (M_0) [kNm]	370	370	370	370	370	370
	Seismic (M) [kNm]	382	384	390	382	393	477
	Δ [%]	3	4	6	3	6	29
750	Static (M_0) [kNm]	312	312	312	312	312	312
	Seismic (M) [kNm]	315	327	318	321	327	381
	Δ [%]	1	5	2	3	5	22

The comparison of the results obtained form the first and second approach has highlighted that the relative displacements calculated using non-linear analysis are larger than those derived from the equivalent linear analysis. Consequently, also the increase of the bending moment acting on the RC retaining walls follows this trend, as possible to see in Table 9 where EL indicates the equivalent linear analysis and NL the non-linear analysis.

It is possible to notice that the difference (Δ) of the bending moment value evaluated in the section located in correspondence to the central slab calculated through the non-linear (NL) analysis and those obtained from the execution of equivalent linear (EL) analysis lies between 2% and 4% for the five natural accelerograms. This limited difference is due to the incidence of the value of bending moment obtained under static conditions on the final value of bending moment compared to the increment due to the seismic load. This situation does not occur considering Lima seismic input where the difference obtained is greater than 40% for the soil profile having shear wave velocity equal to 360 m/s and 450 m/s and almost equal to 20% considering the soil profile characterized by V_S = 600 m/s and V_S = 750 m/s. The significant difference is due to the different characteristics of the Lima seismic signal when compared with those of the other natural accelerograms used in this work. As a matter of fact, it can be noted from Figures 4 and 5 that the duration and the significant part of the Lima seismic signal are much larger than those of the other natural accelerograms. Consequently, as it can be observed from Table 2, also the value of Arias Intensity (strictly related to the seismic signal energy content) of the Lima seismic input is about 3 times the value of the Montenegro seismic input and about 10 times the values of the other natural accelerograms. Moreover, the relevant energy content of the Lima seismic input is mainly located in correspondence with the soil profiles first fundamental frequency, as shown in Figure 5, thus amplifying the resonance effects. On the other hand, the natural accelerograms present peaks also in correspondence with other frequencies, thereby mostly distributing the energy content of the signals.

Table 9. Comparison of the results.

Soil profile (V_s) [m/s]		Montenegro	L'Aquila	Greece	Friuli	Amatrice	Lima
360	EL [kNm]	628	562	601	542	557	619
	NL [kNm]	643	574	616	554	571	875
	Δ [%]	2	2	2	2	3	41
450	EL [kNm]	472	475	532	466	484	520
	NL [kNm]	490	481	541	475	499	769
	Δ [%]	4	1	2	2	3	48
600	EL [kNm]	376	376	379	376	385	387
	NL [kNm]	382	384	390	382	393	477
	Δ [%]	2	2	3	2	2	23
750	EL [kNm]	315	318	315	318	318	315
	NL [kNm]	315	327	318	321	327	381
	Δ [%]	0	3	1	1	3	21

6. Conclusion

In this research work the evaluation of the seismic behavior of a shallow multi-propped underground structure embedded in a dry coarse soil has been investigated through decoupled approaches. The sensitivity analysis has been carried out considering 6 different seismic inputs and 4 soil profiles characterized by different values of shear stiffness modulus related to the shear wave velocity ranging between 360 and 750 m/s. Two different types of analysis (equivalent linear analysis and non-linear analysis) have been carried out to evaluate the soil profile displacements at depth, from the top to the bottom of the retaining wall, in a free-field condition, without taking into account the effects of the presence of the structure. The results show that the relative displacements calculated using non-linear analysis are larger than those derived from the equivalent linear analysis due to the effects of non-linear behavior of the soil. Furthermore, also the seismic increments of bending moment acting on the RC retaining walls follow this trend. In particular, the difference of the maximum bending moment value evaluated in the section located in correspondence to the central slab calculated through the non-linear analysis and those obtained from the equivalent linear analyses is quite low and lies in between 2% and 4% for the 5 natural accelerograms; this is partly due to the high incidence of the static bending moment on the final value of bending moment as compared to the increment due to seismic actions. This is not the case when considering Lima seismic input: the difference is significant especially for the soil profiles characterized by low values of the shear modulus.

Finally, it is important to highlight that the results obtained in this work are related to the specific geometrical features of the structure under study: more generalized results can be obtained considering different types of structural configurations.

7. References

Andreotti G, Lai G.G. (2015). Methodology to derive damage state-dependent fragility curves of underground tunnels, *Proceedings of the 6th international conference on earthquake geotechnical engineering*, Christchurch, New Zealand.

Bickel J.O. (1996). *Tunnel engineering handbook*, 1st Ed., New York: Chapman and Hall.

Bobet A. (2003). Effect of pore water pressure on tunnel support during static and seismic loading, *Tunnelling and Underground Space Technology*, 18(4): 377-393.

Bobet A. (2010). Drained and undrained response of deep tunnels subjected to far-field shear loading, *Tunnelling and Underground Space Technology*, 25(1): 21-31.

Dowding C.H., Rozen A. (1978). Damage to rock tunnels from earthquake shaking, *ASCE Journal of Geotechnical Engineering Division*, 104: 175-191.

Gomez-Masso A., Attala I. (1984). Finite element vs simplified method in the seismic analysis of underground structures, *Earthquake Engineering and Structural Dynamics*, 12: 347-367.

Hashash Y.M.A., Hook J., Schmidt B., Yao J. (2001). Seismic design and analysis of underground structures, *Tunnelling and Underground Space Technology*, 16: 247-293.

Hashash Y.M.A., Musgrove M.I., Harmon J.A., Groholski D.R., Phillips C.A., Park D. (2016). *DEEPSOIL 6.1, User Manual*, Urbana, IL, Board of Trustees of University of Illinois at Urbana-Champaign.

Hoeg K. (1968). Stresses against underground structural cylinders, *ASCE Journal of Soil Mechanics and Foundations Division*, 94: 833-858.

Iida H., Hiroto T., Yoshida N., Iwafuji M. (1996). Damage to Daikai subway station, *Soils and Foundations*, 36: 283-300.

ISO (International Organization for Standardization). (2005). ISO 23469: *Bases for design of structures - Seismic actions for designing geotechnical works. International Standard ISO TC98/SC3/WG10*, Geneva: International Organization for Standardization.

Itasca Consulting Group Inc., 2007 FLAC 2D: Fast Legrangian Analysis of Continua.

JRA (Japan Road Association). (1992). *Guide specifications of design and construction of underground parking lots*, Tokyo: Ministry of Transportation.

Kawashima K. (2000). Seismic design of underground structures in soft ground: A review. *Geotechnical aspects of underground construction in soft ground*. Rotterdam: Balkema.

Kawashima K. (2006). Seismic analysis of underground structures, *Journal of Disaster Research*, 1(3): 378-389.

Kiyomiya O. (1995). Earthquake-resistant design features of immersed tunnels in Japan, *Tunnelling and Underground Space Technology*, 10(4): 463-475

Kontoe S., Zdravkovic L., Potts D., Mentiki C. (2008). Case study on seismic tunnels response. *Canadian Geotechnical Journal*, 45: 1743-1764.

Kuasel E., Christian J.T., Roesset J.M. (1976). Nonlinear behaviour in soil-structure interaction. *ASCE Journal of Geotechnical Engineering Division*, 102(11): 1159-1170.

Kuhlemeyer R. L., Lysmer J. (1973). Finite element method accuracy for wave propagation problems, *ASCE Journal of Soil Mechanics & Foundations Division*, 99: 421-427.

Owen G.N., Scholl R.E. (1981). Earthquake engineering of large underground structures, *Federal Highway Administration and National Science Foundation*, Report No. FHWA/RD-80/195.

Pagliaroli A., Lanzo G., Sanò T. (2007). Confronto fra tre codici di calcolo 2D della risposta sismica locale, *Proceedings of XII Congresso Nazionale "l'Ingegneria sismica in Italia"*, Pisa, Italy.

Park K.H., Tantayopin K., Tontavanich B., Owatsiriwong A. (2009). Analytical solution for seismic-induces ovaling of circular tunnel lining under no-slip interface conditions: A revisit, *Tunnelling and Underground Space Technology*, 24(2): 231-235.

Penzien J, Wu C. (1998). Stresses in linings of bored tunnels, *Earthquake Engineering and Structural Dynamics*, 27: 283-300.

Penzien J. (2000). Seismically induced racking of tunnels lining, *Earthquake Engineering and Structural Dynamics*, 27: 683-691.

Power M., Rosidi D., Keneshiro J., Gilstrap S., Chiou S.J. (1998). Summary and evaluation procedures for the seismic design of tunnels, *Buffalo: National center for earthquake engineering research*, Final report task 112-d-5.3(c).

Seed H.B., Idriss I.M. (1970). Soil moduli and damping factors for dynamic analysis, *Report No. EERC 70-10*, University of California, Berkeley.

Sharma S., Judd W.R. (1991). Underground opening damage from earthquakes, *Engineering Geology*, 30: 262-279.

Soccodato F.M., Tropeano G. (2015). The role of ground motion characters on the dynamic performance of propped retaining structures, *Proceeding of 6th International Conference on Earthquake Geotechnical Engineering*, Christchurch, New Zealand.

St. John C.M., Zahrah T.F. (1987). Aseismic design of underground structures, *Tunnelling and Underground Space Technology*, 2(2): 165-197.

Stokoe K.H., Jung M.J., Menq F.Y., Liao T., Massoudi N., McHood M. (2013). Normalized shear modulus of compacted gravel, *Proceedings of 18th International Conference on Soil Mechanics and Geotechnical Engineering*, Paris, France.

Wang J.N. (1993). *Seismic Design of Tunnels*, 1st Ed, New York: Parson Brinckerhoff Inc.

Wang W.L., Wang T.T., Su J.J., Lin C.H., Seng C.R., Huang T.H. (2001). Assessment of damage in mountain tunnels due to the Taiwan Chi-Chi earthquake, *Tunnelling and Underground Space Technology*, 16: 133-150.

Wang Z.Z., Gao B., Jiang Y.J., Yuan S. (2009). Investigation and assessment on mountain tunnels and geotechnical damage after the Wenchuan earthquake, *Science in China, Series E-Technological Sciences*, 52(2): 546-558.

Yoshiwa K., Fikuchi G. (1984). Earthquake damage to railway tunnels in Japan, *Advances in Tunnelling Technology and Subsurface Use*, 4(3): 75-83.